RASĀYAN *J. Chem.*
Vol. 18 | No. 4 |1927-1933| October-December | 2025
ISSN: 0974-1496 | e-ISSN: 0976-0083 | CODEN: RJCABP
http://www.rasayanjournal.com
http://www.rasayanjournal.co.in

A MECHANISTIC DFT INVESTIGATION OF KETENE AND SILYLKETENE FORMATION FROM CORRESPONDING 1-ALKYNYL ETHERS

J. Tyagi[1], R. Mishra[2] and S. K. Mishra[1,✉]
[1]Department of Chemistry, Zakir Husain Delhi College, University of Delhi, Delhi 110002
[2]Department of Chemistry, Deshbandhu College, University of Delhi, Delhi-110019
✉Corresponding author: drsanjeevkmishra@zh.du.ac.in

ABSTRACT

The present work, using DFT calculations, explores the formation of ketenes from their corresponding alkoxyacetylenes via two paths. Path I discusses the formation of ketene from ethoxyacetylene, and Path II explores the formation of silylketene from ethoxy(silyl)acetylene. Frequency calculations of transition states give only one imaginary frequency with a magnitude more than 500 for both paths, establishing an acceptable transition state in each path. Data from ρ_c and $\nabla^2\rho_c$ calculations further established the mechanism of the two reaction paths. Electronic distribution and its changes in the course of reaction are also explored using NBO analysis, and natural atomic charges are obtained. Reaction energy profile against the reaction coordinate is plotted for both paths. Energetics of the two reactions studied found both the reactions to be exothermic in nature, and the values of activation energy and energy of reaction had a small difference. Furthermore, Path I is found to be more exothermic as compared to Path II. This study finds its importance owing to the fact that the product ketene is susceptible to [2+2] cycloaddition with the reactant itself, which makes the calculation of activation energy and ΔE experimentally difficult. The results of the current study are in accordance with some of the partial theoretical studies done at lower levels of calculation.

Keywords: NBO Analysis, B3LYP, Ethoxyacetylene, Ethoxy(Silyl)Acetylene, Transition State, Thermolysis, Intrinsic Reaction Coordinate (IRC)

RASĀYAN *J. Chem.*, Vol. 18, No. 4, 2025

INTRODUCTION

When experimental studies are difficult to carry out then computational studies shed some light to search for the path! The current study is an addition to this fact since $H_3SiC(H)=C=O$, the simplest silylketene is not a stable molecule and has a tendency to react with the reactant itself. However, computational studies can be very useful to understand the reaction mechanism for such molecules. The ketene family, a group of organic compounds that are used in many synthesis processes, was first discovered by Hermann Staudinger, a German chemist, in 1905.[1] However, silylketene (substituted) formation was achieved much later in the year 1964 by Shchukovskaya, who prepared trimethylsilylketene for the first time by carrying out thermolysis of ethoxy(trimethylsilyl)acetylene.[2] Ketenes are a class of compounds having cumulated double bonds on a central carbon atom (C=C=O) without a pi system being conjugated. Ketenes that have hydrogen on the terminal carbon are thermally unstable and are prone to dimerization, and are difficult to isolate. The experimental synthesis and mechanistic explorations for the synthesis of ketenes have been carried out from different reagents and also from the 1-alkynyl ethers. The detailed discussion on the ketene has been reviewed by Allen and Tidwell in a review.[3,4] 1-alkynyl ethers having hydrogen at the β position are thermally unstable, and they readily dissociate into corresponding ketene and olefin. The reactivity of this reaction is proportional to the number of hydrogens present at the β position. The thermolysis reaction with a silyl group gives silylketenes. The hyperconjugation effect of the silyl group on the terminal carbon makes silylketene stable and isolable. Silylketenes are important and versatile organic reagents and have high synthetic value. These compounds find their uses in many synthesis reactions. Nucleophilic additions of carbon and other heteroatoms, the Wittig reaction, and [2+2] cycloaddition with a carbonyl group in the presence of a Lewis acid are a few to name.[5] The simplest silylketene, i.e., $H_3SiC(H)=C=O$, is difficult to synthesize from a thermodynamic point of view. Furthermore, this is also kinetically unstable to water and oxygen, which makes the synthesis process very difficult and challenging. However, the synthesis of this

http://doi.org/10.31788/RJC.2025.1849395

silylketene in the gas phase was realized in the year 2017 by Tarczay *et al*., who have reported experimental and theoretical calculations for the same.[6] Both theoretical, viz., semi-empirical and ab initio, and experimental investigations on silylketenes have been reported in various studies.[7-11] The current DFT study of the reaction of ethoxyacetylene and ethoxy(silyl)acetylene going under thermolysis in the vacuum phase has been studied to shed more light on the mechanistic path of the two reactions. This study will provide a better understanding of the two formation reactions of ketenes and, thus, contribute to quality education (SDG-4).

EXPERIMENITAL

Method of Calculations

DFT study at the B3LYP/6-311++G(d,p) level has been used to study all the systems, viz., reactants, products, and transition states (TS).[12-14] All the calculations were done using the quantum-based GAUSSIAN-09 package. The optimized geometries of the reactants, products, and corresponding TS have been obtained using the above method. To investigate the reaction mechanism further, changes in bond densities, i.e., ρ_c (electronic charge density) and corresponding $\nabla^2\rho_c$ (Laplacian density), were calculated.[15] This was done using the AIM command on the final optimized geometry. Natural bond order (NBO) analysis was carried out to calculate natural atomic charges in the reactant, TS, and the products. It further helped to explore the changes in electron distribution during the reaction. Stationary points were established using calculated harmonic vibrational frequencies.[16] The transition state was further studied by Intrinsic Reaction Coordinate (IRC) calculation. Reaction energetics was explored by calculating E_a (activation energy) and ΔE (energy of reaction).[17-20] Calculations using HF having the same basis set (6-311++G(d,p)) were also carried out to have a comparative account of the energetics of the reactions discussed here.

RESULTS AND DISCUSSIONS

Structures of Reactants, Transition States, and Products

1-Alkynyl ether converting to ketene and alkene has been studied via two paths, viz., Path I and Path II. The general outline of the reaction paths is depicted in Fig.-1. Figure-2 elaborates the two paths, giving the geometry of the reactant, products, and the TS involved. Table-1 lists the selected geometrical parameters of optimized geometry for all the structures using the B3LYP/6-311++G(d,p) method.

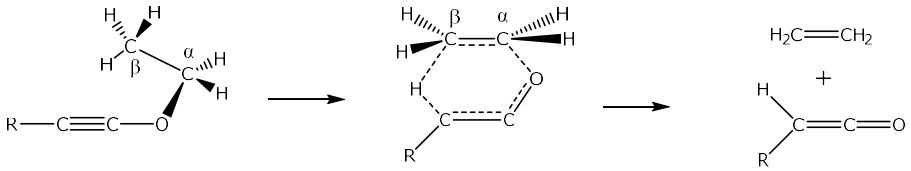

Path I: R = H
Path II: R = SiH_3

Fig.-1: Thermolysis Reaction of 1-Alkynyl Ether to Ketene and Alkene

Formation of Ketene from Ethoxyacetylene (Path I)

Ethoxyacetylene (‘1’) converts to ketene (‘2A’) and the corresponding alkene (‘2B’) via transition state (‘TS12’), as shown in Fig.-2. As the TS forms, there is a significant decrease in the O1-C2-C3 bond angle from 178° to 159°. Also, the C2-O1-C5 and O1-C5-C4 bond angles decrease to a small extent as the TS formation takes place. The bond angle C2-C3-H9 of 82.2° is observed in ‘TS12’ as compared to no bond angle in the reactant (‘1’). The bond lengths of O1-C5 and C4-H9 increase as we go from ‘1’ to ‘TS12’. This indicates a decrease in bond strength, which is also supported by the decrease in the value of bond density ($\rho(r_c)$) in AIM calculation (Table-2). Calculations also show that the $\nabla^2\rho_c$ value for the O1-C5 bond changes from a negative to a positive value as we move from ‘1’ to ‘TS12’, indicating a shift from covalent to non-covalent character. $\nabla^2\rho_c$ values in the case of C4-H9 are negative in both ‘1’ and ‘TS12’, but the increase in the value in TS suggests a decrease in covalent character. A distance of 1.639 Å is observed between C3 and H9 in the ‘TS12’ as compared to no bond between the two atoms in ‘1’, indicating the formation of a six-membered TS. This observation of bond formation is further supported by the $\rho(r_c)$ and $\nabla^2\rho_c$ for the C3-H9 bond (Table-2). The transition state ‘TS12’ is a six-membered planar structure, which is confirmed from the dihedral angle O1-C5-C4-H9 (0°) and H9-C3-C2-O1 (0°). The presence of a single

negative (imaginary) vibrational frequency (Table-4) along with the IRC plot (Fig.-3) points towards an acceptable TS. NBO analysis gives the natural atomic charges, which are listed in Table-3. We can observe that a negative charge builds up at C4 and C3 as we go from '1' to 'TS12'. This is expected and is in synchronization with the process of migration of hydrogen from C4 to C3. Furthermore, the negative charge on C5 increases in 'TS12' when compared to that in '1' due to the noticeable bond lengthening of the O1-C5 bond by 0.629 Å.

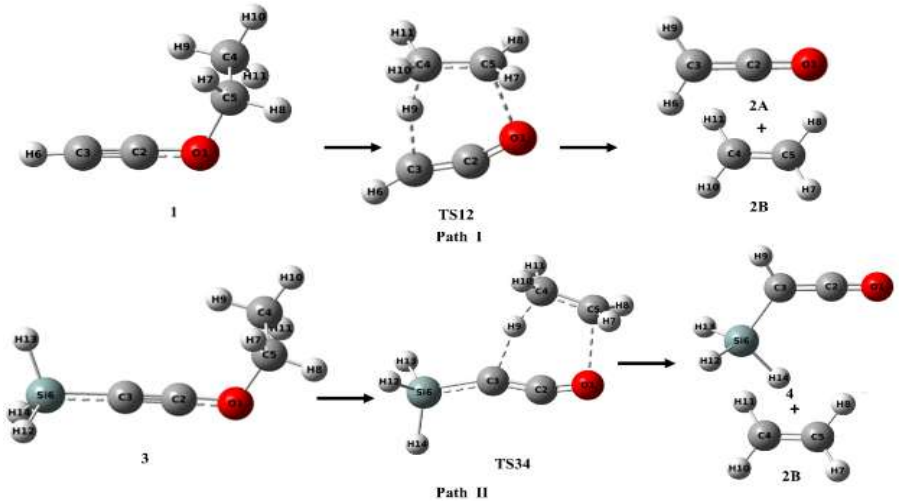

Fig.-2: Optimized Geometry of Reactants, Products, and Transition State for Path I and Path II

Formation of Silylketene from Ethoxy(silyl)acetylene (Path II)

Path II studies the effect of silyl substitution at the C3 position in Ethoxyacetylene ('1'), resulting in Ethoxy(silyl)acetylene ('3'), which converts to silylketene ('4') and the corresponding alkene ('2B') via transition state ('TS34'), as shown in Fig.-2. We observed a substantial decrease in the O1-C2-C3 bond angle from 180° to 162° and some small changes in the other bond angles as the six-membered TS is formed (Table-1). In the 'TS34', a bond angle C2-C3-H9 of ca. 80° is also observed, similar to that in 'TS12'. As in Path I, the bond lengths of O1-C5 and C4-H9 also increase, and the $\rho(r_c)$ magnitude decreases as the reaction proceeds from '3' to 'TS34' in Path II, indicating a decrease in the bond strength (Table-2). A change in the $\nabla^2\rho_c$ value from negative to positive for the O1-C5 bond as we move from '3' to 'TS34' indicates a shift towards non-covalent character from a covalent one. Similar to Path I, the $\nabla^2\rho_c$ value of the C4-H9 bond in Path II is also negative for both '3' and 'TS34', but an increase in the magnitude in TS indicates a decrease in covalent character. The six-membered TS obtained in Path II is also found to be planar. This observation can be confirmed by the two dihedral angles, i.e., O1-C5-C4-H9 (0°) and H9-C3-C2-O1 (0°). The IRC plot (Fig.-3) and presence of a single negative vibrational frequency (Table-4) establish the presence of a valid TS.

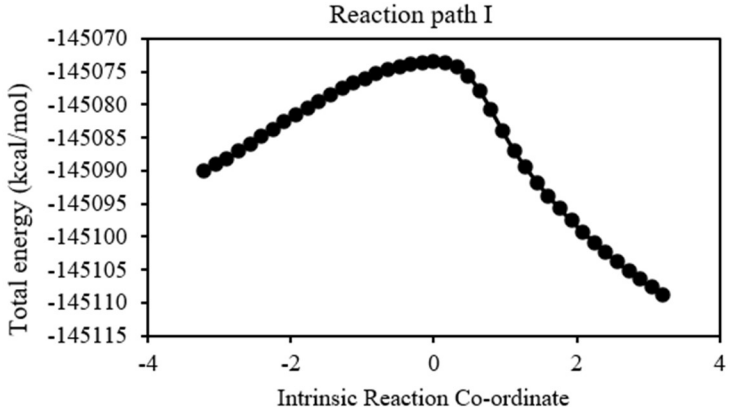

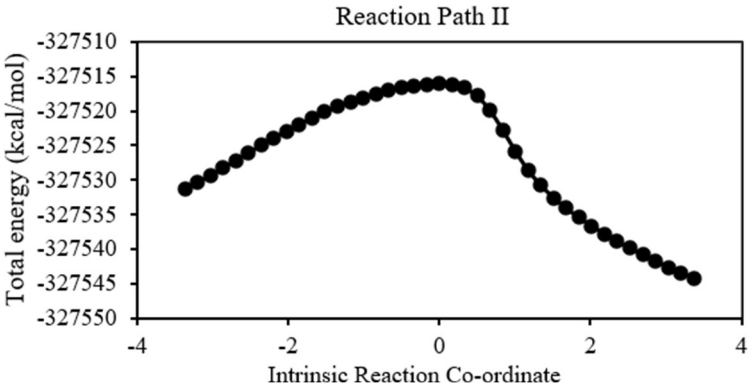

Fig.-3: Potential Energy Profile (PES) for Reaction Path I and Path II. Zero Point Represents the Transition State along the IRC. The Negative Represents the Reactant, and the Products are towards Positive Directions. B3LYP/6-311G++ (d, p) Method was used for the Calculation

The changes in the bonding parameter are also evident from the NBO analysis, giving natural atomic charges (Table-3). Our observations revealed that a negative charge builds up at C3 and C4 as we go from '3' to 'TS34', suggesting migration of hydrogen from C4 to C3. The charge on C5 is found to be increased in 'TS34' when compared to that in '3'; this observation is similar to that in Path I due to the same reason, i.e., bond lengthening of O1-C5 by a considerable magnitude of 0.730 Å. The silyl group substitution effect on the reaction Path II is visible in bonding parameters. If we compare C3 in '1' and '3', we find a substantial increase in the negative charge. This would, in turn, facilitate the transfer of H9, which is reflected in the energetics of the reaction paths and would be discussed in a later section of the paper.

Table-1: Selected Geometric Parameters using B3LYP/6-311++G(d,p) of Reactants ('1' and '3'), Products ('2A', '2B' and '4') and Transition States ('TS12' and 'TS34')

System[b]	1	TS12	2A	2B	3	TS34	4
Bond Lengths (in Å)							
O1-C2	1.296	1.216	1.161	-	1.430	1.208	1.161
C2-C3	1.202	1.248	1.310	-	1.210	1.256	1.310
O1-C5	1.464	2.093	-	-	1.430	2.160	-
C4-C5	1.516	1.413	-	1.329	1.540	1.410	-
C4-H9	1.092	1.247	-	-	1.070	1.244	-
C3-H9	-	1.639	1.080	-	-	1.668	1.085
C5-H7	1.093	1.081	-	1.085	1.070	1.081	-
Si6-C3	-	-	-	-	1.940	1.817	1.863
Bond Angles (in Degrees)							
O1-C2-C3	178.2	158.9	180.0	-	180.0	162.2	178.3
C2-O1-C5	116.0	104.4	-	-	109.5	102.7	-
O1-C5-C4	111.2	106.4	-	-	109.5	105.1	-
C5-C4-H9	111.1	105.2	-	-	109.5	105.2	-
H7-C5-C4	112.0	121.0	-	121.7	109.5	121.3	-
C2-C3-H9	-	82.2	119.7	-	-	79.8	116.8
H14-Si6-C3	-	-	-	-	109.5	109.6	108.3
Dihedral Angles (in Degrees)							
O1-C5-C4-H9	61.9	0.0	-	-	60.0	0.0	-
H9-C3-C2-O1	-	0.0	180.0	-	-	0.0	179.8
H7-C5-C4-H11	179.6	12.9	-	180.0	-180.0	152.3	-
C3-C2-O1-C5	-168.9	0.0	-	-	60.0	0.0	-
Si6-C3-C2-O1	-	-	-	-	180.0	180.0	-

Table-2: Some Selected Bonding Characteristics of Reaction Paths using B3LYP/6-311++G(d,p) Optimized Geometry

Path I						
System[a]	1		TS12		2A	
	$\rho(r_c)$	$\nabla^2\rho_c$	$\rho(r_c)$	$\nabla^2\rho_c$	$\rho(r_c)$	$\nabla^2\rho_c$
C2-C3	0.392	-0.955	0.367	-0.936	0.301	-0.704
O1- C2	0.330	-0.354	0.398	-0.090	0.374	-0.514
O1-C5	0.222	-0.330	0.055	0.121	-	-
C4-C5	0.251	-0.595	0.297	-0.806	-	-
C3-H9	-	-	0.075	0.026	0.280	-0.956
C4-H9	0.275	-0.918	0.181	-0.376	-	-
Path II						
System[a]	3		TS34		4	
	$\rho(r_c)$	$\nabla^2\rho_c$	$\rho(r_c)$	$\nabla^2\rho_c$	$\rho(r_c)$	$\nabla^2\rho_c$
C2-C3	0.384	-0.865	0.374	-0.881	0.326	-0.678
O1- C2	0.334	-0.334	0.425	-0.058	0.455	0.178
O1-C5	0.219	-0.316	0.043	0.110	-	-
C4-C5	0.251	-0.597	0.308	-0.860	-	-
C3-H9	-	-	0.076	0.028	0.266	-0.855
C4-H9	0.275	-0.918	0.167	-0.318	-	-

ρ_c in e/au^3 and $\nabla^2\rho_c$ in e/au^5

Table-3: Natural Atomic Charges

System[a]	1	TS12	2A	2B	3	TS34	4
O1	-0.528	-0.536	-0.442	-	-0.517	-0.524	-0.443
C2	0.306	0.466	0.696	-	0.369	0.514	0.719
C3	-0.383	-0.546	-0.763	-	-0.621	-0.797	-0.976
C4	-0.609	-0.665	-	-0.366	-0.609	-0.669	-
C5	-0.010	-0.106	-	-0.366	-0.011	-0.102	-
H9	0.214	0.284	0.254	-	0.215	0.303	-
Si6	-	-	-	-	0.807	0.897	0.906

Harmonic Vibrational Frequencies

Vibrational frequencies along with the intensities for the reactant, product, and the corresponding TS for both the reaction paths studied here are tabulated in Table-4. The B3LYP/6-311++G(d,p) method is used for these calculations. Our calculations result in positive vibrational frequencies for reactants and products in both paths, indicating stable geometries. Furthermore, 'TS12' in Path I and 'TS34' in Path II possess a single imaginary frequency with magnitude >500, establishing an acceptable transition state. The zero-point vibrational energies (ZPVE) are also calculated using the aforementioned method and are reported in Table-4.

Table-4: Calculated Harmonic Vibrational Frequencies[a] (cm^{-1}) and ZPVE (kcal mol^{-1}) using B3LYP/6-311G++(d,p) Optimized Geometry[b]

Path I					
1		TS12		2A	2B
441 (32)	1163 (53)	607i (198)	1320 (123)	538 (35)	943 (112)
522 (47)	1373 (20)	233 (98)	1388 (101)	581 (107)	3118 (26)
628 (62)	2183 (235)	304 (29)	1425 (26)	2150 (693)	
954 (21)	2955 (30)	604 (36)	1505 (52)	3074 (30)	
1065 (23)	3030 (29)	620 (65)	2043 (248)		
1089 (152)	3381 (111)	802 (109)	3317 (69)		
ZPVE					
55.8		51.5		19.8	31.9
Path II					
3		TS34		4	
484 (38)	1373 (20)	501i (212)	1438 (74)	412 (31)	
592 (51)	2152 (124)	278 (21)	1519 (90)	595 (23)	

666 (58)	2152 (122)	405 (71)	2070 (618)	672 (86)
671 (57)	2155 (218)	549 (95)	2137 (134)	776 (49)
785 (22)	2217 (491)	646 (81)	2147 (88)	915 (51)
809 (58)	2959 (29)	668 (50)	2154 (89)	916 (276)
919 (423)	3033 (28)	787 (102)		946 (116)
925 (65)		914 (52)		1045 (30)
932 (82)		916 (412)		1275 (39)
964 (51)		944 (118)		2129 (973)
1198 (94)		1284 (117)		2152 (126)
1278 (29)		1349 (34)		2171 (182)
ZPVE				
66.0		62.0		30.4

a. Scaled by 0.9679 b. See Fig.-2
c. Values in the parenthesis are intensities in km/mol

Energetics of the Two Reaction Paths (I and II)

Table-5 lists the activation energy (E_a) and energy of reaction (ΔE) for Path I and Path II. The B3LYP/6-311++G(d,p) method is used for the calculation. HF/6-311++G(d,p) calculations are also done to compare the results. The product ketene, obtained readily, reacts with the reactants still remaining and undergoes [2+2] cycloaddition for both paths. This ongoing side reaction makes the experimental estimation of the enthalpy difficult and thus has not been reported. The lower value of the calculated enthalpy establishes the fact. Both reactions are exothermic in nature. The ΔE value for Path II is found to be less exothermic than that for Path I. E_a and ΔE obtained by Oblin *et al*., who used the MP2/6-31++G** method, were lower as compared to our calculation at both the HF and B3LYP levels.[9] The activation energy of Path I is slightly higher than that of Path II. This may be attributed to the fact that there is a buildup of more negative charge at C3 in '3' due to the silyl group, thus facilitating the transfer of H9 more easily. If we compare the results of HF and B3LYP methods, the inclusion of electron correlation results in a decrease in ΔE values.

Table-5: Calculated Activation Energies (E_a) and Energy of Reaction (ΔE) (in kcal mol^{-1}) for Path I and Path II

Reaction[a]		A	B	Others[b]
Path I	E_a	49.3	24.2	30.9
	ΔE	-24.2	-24.4	-11.6
Path II	E_a	47.2	23.7	32.3
	ΔE	-19.5	-19.9	-10.5

A. HF/6-311++G(d,p) optimized geometry; B. B3LYP/6-311++G(d,p) optimized geometry

CONCLUSION

Formation of ketene and silylketene from their corresponding alkoxyacetylene is discussed in reaction Path I and Path II, respectively. Both reactions are found to be exothermic, with Path II being less exothermic as compared to Path I. Both the reaction paths involved a six-member planar structure, though not regular. A valid transition state is obtained in both paths. This fact is established by a single imaginary frequency with a magnitude of over 500. From the energetics of the reactions, we have observed that the difference in the ΔE (~ 4.7 kcal/mol) is not much in the two reaction paths. Also, the E_a of the two reactions is similar, with a difference of only ~ 2 kcal/mol. The presence of a silyl group (-SiH3) in Path II facilitates the ketene formation and also enhances the stability of ketene. Cyclization of reactants into the transition state and subsequent dissociation into the products are supported by the ρ_c, $\nabla^2\rho_c$, and natural atomic charge values. On comparing the B3LYP and HF methods, we can conclude that DFT calculations include the exchange and correlation and give good results at low computational cost. The theoretical investigation of these reaction paths also becomes important here, as the product ketene is prone to [2+2] cycloaddition with the reactant itself, thus making the determination of E_a as well as ΔE experimentally difficult. This study will help in understanding the mechanistic path of the two reactions, and it will further aid in quality education, which is one of the SDGs.

ACKNOWLEDGEMENTS

The authors would like to acknowledge Zakir Husain Delhi College, Deshbandhu College, and the University of Delhi for providing the necessary resources for the present work.

CONFLICT OF INTERESTS

All the authors declare that there is no conflict of interest.

AUTHOR CONTRIBUTIONS

The present work is related to *SDG-4: Quality Education*. All the authors contributed significantly to this manuscript, participated in reviewing/editing and approved the final draft for publication. The research profile of the authors can be verified from their ORCID ids, given below:

Sanjeev Kumar Mishra https://orcid.org/0009-0006-1555-3128
Joyti Tyagi https://orcid.org/0000-0002-2689-8440
Ruby Mishra https://orcid.org/0000-0002-1305-4177

REFERENCES

1. H. Staudinger, *Chemische Berichte*, **38**, 1735(1905), https://doi.org/10.1002/cber.19050380283
2. L. L. Shchukovskaya, R. I. Pal'chilk and A. N. Lazarev, *Doklady Akademii Nauk SSSR*, **164**, 357(1965)
3. A. D. Allen and T. T. Tidwell, *Arkivoc*, **2016**, 415(2016), https://doi.org/10.24820/ark.5550190.p009.634
4. T. T. Tidwell, *European Journal of Organic Chemistry*, **2006**, 563(2006), https://doi.org/10.1002/ejoc.200500452
5. A. Pommier, P. Kocienski and J. M. Pons, *Journal of the Chemical Society, Perkin Transactions,* **1**, 2105(1998), https://doi.org/10.1039/A801254G
6. G. Tarczay, M. Förstel, S. Góbi, P. Maksyutenko and R. I. Kaiser, *ChemPhysChem*, **18**, 882(2017), https://doi.org/10.1002/cphc.201601422
7. H. Sakurai, A. Shirahata, K. Sasaki and A. Hosomi, *Synthesis*, **1979**, 740(1979), https://doi.org/10.1055/s-1979-28823
8. A. Moyano, M. A. Pericas, F. Serratosa, and E. Valenti, *The Journal of Organic Chemistry*, **52**, 5532(1987), https://doi.org/10.1021/jo00234a007
9. M. Oblin, M. Rajzmann and J. M. Pons, *Tetrahedron*, **53**, 8165(1997), https://doi.org/10.1016/S0040-4020(97)00503-6
10. M. Oblin, F. Fotiadu, M. Rajzmann, and J. M. Pons, *Journal of the Chemical Society, Perkin Transactions,* **2**, 1621(1997), https://doi.org/10.1039/A703439C
11. A. D. Allen, T. T Tidwell, *Tetrahedron Letters*, **32**, 847(1991), https://doi.org/10.1016/S0040-4039(00)92101-4
12. A. D. Becke, *Physical Review A*, **38**, 3098(1988), https://link.aps.org/doi/10.1103/PhysRevA.38.3098
13. A. D. Becke, *Journal of Chemical Physics*, **98**, 5648(1993), https://doi.org/10.1063/1.464913
14. C. Lee, W. Yang and R. G. Parr, *Physical Review B*, **37**, 785(1988), https://doi.org/10.1103/PhysRevB.37.785
15. R. F. W. Bader, *Accounts of Chemical Research*, **18**, 9(1985), https://doi.org/10.1021/ar00109a003
16. M. P. Andersson and P. Uvdal, *The Journal of Physical Chemistry A*, **109**, 2937(2005), https://doi.org/10.1021/jp045733a
17. W. J. Hehre, L. Radom, P. R. Schleyer and J. A. Pople, Ab-initio Molecular Orbital Theory, John Wiley, New York, pp. 548 (1986), https://doi.org/10.1002/jcc.540070314
18. R. G. Parr and W. Yang, Density Functional theory of Atoms and Molecules, Oxford University Press, New York, Oxford, pp. IX+333 (1989), https://doi.org/10.1002/qua.560470107
19. J. K. Labanoeski and J. W. Andzelin, Density Functional Methods in Chemistry, Springer Verlag, New York (1991), https://doi.org/10.1007/978-1-4612-3136-3
20. S. H. Vosko, L. Wilk, and M. Nusair, *Canadian Journal of Physics*, **58**, 1200(1980), https://doi.org/10.1139/p80-159

[RJC-9395/2025]